

Submitted to the Astronomical Journal

Far Ultraviolet Observations of the Dwarf Novae SS Aur and RU Peg in Quiescence

Edward M. Sion, Fuhua Cheng, Patrick Godon¹, Joel A. Urban

*Astronomy and Astrophysics, Villanova University,
800 Lancaster Avenue, Villanova, PA 19085, USA*

patrick.godon@villanova.edu edward.sion@villanova.edu, fcheng@ast.vill.edu,
jurban@ast.vill.edu

Paula Szkody

Department of Astronomy, University of Washington, Seattle, WA 98195, USA

szkody@alica.astro.washington.edu

ABSTRACT

We have analyzed the Far Ultraviolet Spectroscopic Explorer (FUSE) spectra of two U Gem-Type dwarf novae, SS Aur and RU Peg, observed 28 days and 60 days (respectively) after their last outburst. In both systems the FUSE spectra (905 – 1182 Å) reveal evidence of the underlying accreting white dwarf exposed in the far UV. Our grid of theoretical models yielded a best-fitting photosphere to the FUSE spectra with $T_{eff}=31,000\text{K}$ for SS Aur and $T_{eff}=49,000\text{K}$ for RU Peg. This work provides two more dwarf nova systems with known white dwarf temperatures above the period gap where few are known. The absence of C III (1175 Å) absorption in SS Aur and the elevation of N above solar suggests the possibility that SS Aur represents an additional accreting white dwarf where the surface C/N ratio derives from CNO processing. For RU Peg, the modeling uncertainties prevent any reliable conclusions about the surface abundances and rotational velocity.

Subject headings: accretion, accretion disks - novae, cataclysmic variables - white dwarfs

¹Visiting at the Space Telescope Science Institute, Baltimore, MD 21218, USA

1. Introduction: Accretion Onto White Dwarfs in Dwarf Novae

Dwarf Novae (DN) are a subclass of Cataclysmic Variable (CV) Systems, in which a white dwarf (WD, the primary) accretes hydrogen-rich matter from a low-mass main sequence-like star (the secondary) filling its Roche lobe. The transferred gas forms an accretion disk around the white dwarf, and is subject to a thermal instability that causes cyclic changes of the accretion rate. A low rate accretion ($\approx 10^{-11} M_{\odot} yr^{-1}$) quiescence stage is followed every few weeks to months by a high rate accretion ($\approx 10^{-8} M_{\odot} yr^{-1}$) outburst stage of days to weeks. It is believed that these outbursts (dwarf nova accretion event or nova-like high state), are punctuated every few thousand years or more by a Thermonuclear Runaway (TNR) explosion: the classical nova (Warner 1995).

In some dwarf novae during quiescence, the accretion rate and disk temperature has so greatly declined that the disk emits mainly in the optical and has little or no contribution to the FUV spectrum. Consequently, the underlying hot white dwarf accreter is exposed spectroscopically and dominates the far UV light. We have been studying these systems extensively with HST since we are able to directly observe the physical effects of disk accretion onto the white dwarf. These natural *accretion laboratories* have yielded, for the central accreters, the first rotation rates (due to accretion spinup), T_{eff} 's, cooling rates, chemical abundances of the accreted plus original white dwarf matter, and dynamical and gravitational redshift masses. Unfortunately, the number of such systems above the period gap has been very limited (U Gem and RX And are the only solid cases thus far). It is of considerable interest to find other such systems.

Above the gap, dwarf novae even during quiescence may have accretion rates sufficiently high that an optically thick disk and/or very hot boundary layer dominate their FUV spectra. Moreover, these higher accretion rates would also be expected to produce significant long term heating of the white dwarf accretor. However, for the disk instability model to apply as the mechanism for their dwarf nova outbursts, the mean accretion rate \dot{M} must be lower than the critical rate M_{crit} to trigger the instability. Systems with mean $\dot{M} > M_{crit}$ do not exhibit cyclic changes of \dot{M} (Shafter et al. 1986). An obvious fundamental observational question is: which hot component dominates in the far UV and what are its physical properties?

Among the high \dot{M} U Gem-type systems, two objects, SS Aur and RU Peg, have extensive earlier multi-wavelength studies and reasonably well-constrained distances to represent important test cases. Their dwarf nova behavior parameters are listed in Table 1.

RU Peg has an orbital period $P_{orb} = 0.3746$ days (Stover 1981), a system inclination $i = 33^{\circ}$ (Shafter 1983), a secondary (mass donor) spectral type K2-5V (Wade 1982; Shafter

1983), a primary (WD) mass $M_{wd} = 1.29 \pm 0.20 M_{\odot}$ (Shafter 1983). The near-Chandrasekhar mass for the white dwarf has been corroborated by the Sodium (8190Å) doublet radial velocity study of Friend et al. (1990). They obtained a mass of $1.24 M_{\odot}$ for the white dwarf and also found very good agreement with the solution, including agreement with the range of plausible inclination, found in the study by Stover (1981). Recently, a Hubble FGS parallax of 3.55 ± 0.26 mas was measured by Johnson et al. (2003).

SS Aur has an orbital period $P_{orb} = 0.1828$ days (Shafter & Harkness 1986). The mass of its white dwarf has been estimated to be $M_{wd} = 1.08 \pm 0.40 M_{\odot}$, while its secondary is known to have a mass $M_2 = 0.39 \pm 0.02 M_{\odot}$, and a system inclination $i = 38^{\circ} \pm 16^{\circ}$ (Shafter 1983). SS Aur has an HST FGS parallax measurement of 497 mas (Harrison et al. 1999).

In two recent studies, Lake & Sion (2001) and Sion & Urban (2002) analyzed IUE far UV archival spectra of both systems which revealed they contain very hot white dwarfs. For SS Aur, their best-fit model photosphere has $T_{eff} = 30,000\text{K}$, $\log g = 8.0$, and solar composition abundances, while the best-fit accretion disk model has $M_{wd} = 1.0 M_{\odot}$, $i = 41^{\circ}$, and $\dot{M} = 10^{-10} M_{\odot} \text{yr}^{-1}$. They used a measured parallax (497mas; 201 pc) for SS Aur, from observations with the HST FGS (Harrison et al. 1999), together with the scale factor $S = 1.12 \times 10^{-3}$ from their best fit, to calculate a radius for the emitting source of 4.68×10^8 cm. This radius is clearly that of a compact object, a white dwarf, not an accretion disk.

For RU Peg during quiescence, their best-fit high gravity solar composition photosphere models yielded $T_{eff} = 50 - 53,000\text{K}$ with scale factor distances of ~ 250 parsecs. Optically thick accretion disk models imply accretion rates between $1 \times 10^{-9} M_{\odot} \text{yr}^{-1}$ and $1 \times 10^{-10} M_{\odot} \text{yr}^{-1}$ in order to match the steeply sloping far UV continuum, but yielded distances of 600 to 1300 parsecs, well beyond the estimated distance range of 130 to 300 parsecs (now known to be 282 pc from the new parallax by Johnson et al. (2003)). However, they could not rule out that the far UV energy distribution is due to a multi-temperature white dwarf with cooler, more slowly rotating higher latitudes and a rapidly spinning, hotter equatorial belt.

Is the FUV spectral energy distribution best represented by a model of an accretion disk alone, a composite white accretion disk plus white dwarf, a rapidly spinning accretion belt and high gravity photosphere with an inhomogeneous temperature distribution or by a uniform temperature white dwarf synthetic spectrum alone? We will make use of the parallaxes for both objects to determine the source of the FUV energy distribution. FUSE offers a large variety and broad range of critical line transitions at high spectral resolution across a broad range of ionization states/levels and elements to help us advance our understanding of the physics of the boundary layer and accretion.

2. Observations and Analysis

FUSE is a low-earth orbit satellite, launched in June 1999. Its optical system consists of four optical telescopes (mirrors), each separately connected to a different Rowland spectrograph. The four diffraction gratings of the four Rowland spectrographs produce four independent spectra on two photon counting area detectors. Two mirrors and two gratings are coated with SiC to provide wavelength coverage below 1020 Å, while the other two mirrors and gratings are coated with Al and a LiF overcoat. The Al+LiF coating provides about twice the reflectivity of SiC at wavelengths >1050 Å, and very little reflectivity below 1020 Å (hereafter the SiC1, SiC2, LiF1 and LiF2 channels).

A spectrum of SS Aur in quiescence was taken by FUSE on February 13, 2002 at 07:01 UT (MJD52318) approximately 28 days after the last outburst. The exposure time was 14,513 seconds through the low resolution (LWRS: 30"x30") aperture. A spectrum of RU Peg in quiescence was taken by FUSE on July 4, 2002, at 17:09 UT (MJD52459) approximately 60 days after the last outburst. The exposure time was 1060 seconds through the LWRS aperture. LWRS was used in both cases since it is least prone to slit losses due to the misalignment of the four FUSE telescopes. The calculated S/N of the co-added spectra at 0.1 Å resolution is 3.65 for RU Peg and 4.67 for SS Aur. The S/N improves to ≈ 10 at 0.5 Å resolution. It is clear that the relatively poor FUSE spectral quality of both SS Aur and RU Peg speaks to the requirement for more observing time. For example, SS Aur should have had at least 20,000 sec while for RU Peg, at least 5,000 sec is required.

The data used were reduced with the CalFUSE pipeline version 2.1.6. In this version, event bursts are automatically taken care off. Event bursts are short periods during an exposure when high count rates are registered on one of more detectors. The bursts exhibit a complex pattern on the detector, their cause, however, is yet unknown (it has been confirmed that they are not detector effects). Luckily no event bursts were reported for the present observations. SS Aur, with a flux of $\approx 10^{-14} \text{ergs s}^{-1} \text{cm}^{-2} \text{Å}^{-1}$, is actually a relatively weak source. The minimum acceptable pulse height for ttag FUSE data is controlled by the parameter PHALOW. Increasing this parameter can reduce the internal detector background, which is helpful for spectra of very faint targets (though one has to make sure that "real" photon events are not inadvertently discarded when the threshold is raised). Similarly, one can reduce the maximum acceptable pulse height for ttag FUSE data by reducing the parameter PHAHIGH to a value closer to the tail of the pulse height distribution (here also one has to be cautious to make ensure that "real" events are not removed). For SS Aur, we ran CALFUSE after we slightly increased PHALOW and decreased PHAHIGH in the parameter files **scrn*.fit** to reduce the noise (background events) as explained above.

We combined the individual exposures and channels to create a time-averaged spectrum with a linear, 0.1 \AA dispersion, weightin the flux in each output datum by the exposure time and sensitivity of the input exposure and channel of origin. The details are given here. During, the observations, Fine Error Sensor A, which images the LiF 1 aperture was used to guide the telescope. The spectral regions covered by the spectral channels overlap, and these overlap regions are then used to renormalize the spectra in the SiC1, LiF2, and SiC2 channels to the flux in the LiF1 channel. We then produce a final spectrum that covers almost the full FUSE wavelength range $905 - 1182 \text{ \AA}$. The low sensitivity portions of each channel are discarded. In most channels there exists a narrow dark stripe of decreased flux in the spectra running in the dispersion direction. This stripe has been affectionately known as the "worm" and it can attenuates as much as 50% of the incident light in the affected portions of the spectrum. The worm has been observed to move as much as 2000 pixels during a single orbit in which the target was stationary, and it appears to be present in every exposure and, at this time, there is no explanation for it. Because of the temporal changes in the strength and position of the worm, CALFUSE cannot correct target fluxes for its presence. Here we take particular care to discard the portion of the spectrum where the so-called *worm* 'crawls', which deteriorates LiF1 longward of 1125 \AA . Because of this the $1182 - 1187 \text{ \AA}$ region (covered only by the LiF1 channel) is lost.

We then rescale and combine the spectra. When we combine, we weight according to the area and exposure time for that channel and then rebin onto a common wavelength scale with both a 0.5 \AA (Figures 1 & 2) and a 0.1 \AA (Figures 3 & 4) resolutions. The 0.5 \AA binning is more convenient to identify absorption lines as the spectra are indeed pretty noisy at 0.1 \AA binning.

The FUSE spectrum of SS Aur is displayed in figure 1 where we have identified the strongest absorption features. Table 2 lists in the first column the central wavelength of the line, second column the flux at that wavelength, third column the equivalent width (EW) in Angstroms, fourth column the full-width at half-maximum (FWHM), and the last column the identified ions.

The FUSE spectrum of RU Peg is displayed in figure 2 and the line measurements are given in table 3, where the column headings are the same as for Table 2.

Based upon our expectation that the accreting white dwarf is the dominant source of FUV flux in both systems during quiescence, we carried out a high gravity photosphere synthetic spectral analysis. The model atmosphere (Hubeny 1988, TLUSTY), and spectrum synthesis (Hubeny & Lanz 1995, SYNSPEC) codes and details of our χ^2_ν (χ^2 per degree of freedom) minimization fitting procedures are discussed in detail in Sion et al. (1995) and will not be repeated here. To estimate physical parameters, we took the white dwarf

photospheric temperature T_{eff} , Si and C abundances, and rotational velocity v_{rot} as free parameters. We normalize our fits to 1 solar radius and 1 kiloparsec such that the distance of a source is computed from $d = 1000(pc) * (R_{wd}/R_{\odot})/\sqrt{S}$, or equivalently the scale factor $S = \left(\frac{R_{wd}}{R_{\odot}}\right)^2 \left(\frac{d}{kpc}\right)^{-2}$, is the factor by which the theoretical flux (integrated over the FUSE wavelength range) has to be multiplied to equal the observed (integrated) flux.

In preparation for our model fitting of SS Aur, we masked the following wavelength regions where several narrow emission-like features occur: 959.5 - 950.0 Å, 972.4 - 972.6 Å, 988.6 - 989.0 Å, 1025.2 - 1026.0 Å. For RU Peg, we masked the following wavelength regions : <915 Å, 974 - 980 Å, 1029 - 1037 Å, >1170 Å. We chose to vary the T_{eff} , rotational velocity, and silicon and carbon abundances in our fitting. The grid of models extended over the following range of parameters: $T_{eff}/1000$ (K) = 22, 23, ..., 55; Si = 0.1, 0.2, 0.5, 1.0, 2.0, 5.0; C = 0.1, 0.2, 0.5, 1.0, 2.0, 5.0; and $v_{rot} \sin i$ (km s⁻¹) = 100, 200, 400, 600, 800. Since the distance $d = 201$ pc from the FGS parallax, we used this distance and the reduced χ^2 value to determine the best-fitting model. In addition, as the WD is expected to be massive we fixed $\log g = 9.0$.

For SS Aur, the best fitting model from our χ^2_{ν} minimization routine has the following parameters: $T_{eff}/1000$ (K) = 33 +15/-7 Si = 1.0 +1.0/-0.6 times solar, C = 0.1 +0.9/-0.1 times solar, N = 2.0 +1.8/-0.7, $v_{rot} \sin i = 400 \pm 400$ km s⁻¹, χ^2_{ν} , scale factor = 3.82×10^{-4} . The best-fitting model is displayed in figure 3. This model gives a reasonable agreement with the FUSE continuum distribution and lines but yields a distance of 303 pc or 1.5 times the parallax value. Using the above parameters, the N abundance was found to have an upper limit N<8 times solar.

Next, we tried models of accretion disks alone from the grid of Wade and Hubeny (1998). We fixed the inclination and the white dwarf mass at the published values of 41 degrees with $M_{wd} = 1.2M_{\odot}$. The resulting best-fit had the following parameters: $\chi^2_{\nu} = 2.56$, scale factor = 1.15×10^{-2} and an accretion rate $\dot{M} = 10^{-10}M_{\odot}\text{yr}^{-1}$, corresponding to a distance of 931 pc, or 4.6 times the parallax distance. We conclude that an optically thick accretion disk by itself does not satisfactorily account for the FUSE spectrum.

We assessed the effectiveness of combining an accretion disk with a white dwarf, again fixing the white dwarf mass at $1.2M_{\odot}$, the inclination angle of the disk at 41 degrees. The white dwarf temperature and disk accretion rate were free parameters. For this exercise, the best-fitting combination was the following: $T_{eff} = 27,000\text{K}$, $\dot{M} = 1 \times 10^{-11}M_{\odot}\text{yr}^{-1}$, $\chi^2_{\nu} = 1.85$, scale factor = 5.78 with the accretion disk accounting for 44% of the flux and the white dwarf accounting for 56% of the flux. However, a model-derived distance is 366 pc, larger than the parallax distance by a factor of 2.

Finally, we examined whether a two-temperature white dwarf consisting of a slowly rotating cooler photosphere and a hot rapidly spinning accretion belt would give better agreement with the FUSE data. The best-fitting white dwarf plus accretion belt combination had the following parameters: $T_{eff} = 27,000\text{K}$, $T_{belt} = 48,000\text{K}$, $V_{belt} = 3000 \text{ km/s}$, $\chi^2_\nu = 1.74$, scale factor $= 4.87 \times 10^{-4}$ with the cooler photosphere giving 73% of the FUV light and the accretion belt providing 27%. The scale-factor-derived distance is 267 pc, only a factor of 1.3 larger than the parallax distance.

Thus, based upon the lowest χ^2_ν values achieved and agreement with a distance of 201 pc, we conclude that either a lone single temperature white dwarf with $T_{eff} = 33,000\text{K}$ or a combined white dwarf with $T_{eff} = 27,000\text{K}$ plus an accretion belt with $T_{belt} = 48,000\text{K}$ provide the best agreement with the FUSE spectrum. Models fits with an accretion disk alone or a combined white dwarf plus an accretion disk imply discrepant distances and larger χ^2 values and can be eliminated as the source of the FUSE spectrum.

For RU Peg, we also fixed $M_{wd} = 1.2M_\odot$ because of its published high mass, and fixed $\log g = 9.0$. The FGS parallax of Johnson et al. gives a distance $d = 282 \text{ pc}$. We used this distance and the reduced χ^2_ν value to distinguish which model is the best-fitting among a single temperature white dwarf alone, a steady state, optically thick accretion disk alone, a combined photosphere plus an accretion disk or a two-temperature white dwarf consisting of a cooler, more slowly rotating photosphere and a hot, rapidly spinning accretion belt.

For RU Peg, the best fitting model from our χ^2_ν minimization routine (with 3 sigma error bars) has the following parameters: $T_{eff}/1000 \text{ (K)} = 53 +6/-7$, $\text{Si} = 0.1 +1.0/-0.1$ times solar, $\text{C} = 0.1 +0.9/-0.1$ times solar, an upper limit N abundance of $\text{N} < 8.0$ times solar, $v_{rot} \sin i = 100 +400/-100 \text{ km s}^{-1}$, $\chi^2_\nu = 4.06$, and scale factor $= 5.53 \times 10^{-4}$. This best-fit gave a distance of 263 pc, within about 20 parsecs of the parallax distance. The best-fitting model is displayed in figure 4. Unfortunately, the RU Peg spectrum is under-exposed and therefore the S/N and spectrum quality is less than satisfactory.

For an accretion disk alone, we fixed the inclination angle at 41 degrees, $M_{wd} = 1.2M_\odot$, with the accretion rate a free parameter. We found the best-fitting disk model to have $\dot{M} = 10^{-9}M_\odot\text{yr}^{-1}$ with a $\chi^2_\nu = 4.18$, a scale factor $= 5.57 \times 10^{-3}$ but a distance of 1.34 kpc, clearly erroneous. When we combined white dwarf plus accretion disk models with T_{eff} varying between 36,000 and 60,000K (in steps of 1000K) and \dot{M} varying over the full range of the disk model grid, there was no improvement in the fitting and the scale factor-derived distance was still grossly too large.

Next, we tested two-temperature fits with a cooler, slowly rotating photosphere and a hot, rapidly spinning, equatorial belt as expected from disk accretion. In this experiment, we

varied the WD T_{eff} between 42,000K and 60,00K, the accretion belt temperature between 50,000K and 60,000K in steps of 1000K and kept the C and Si abundances of the white dwarf fixed. Once again, as in the white dwarf plus disk case, there was no improvement in the χ^2_ν value.

3. Results and Discussions

The quality of the model fits to the FUSE spectra of the two systems is quite different. The fit to SS Aur is very much in agreement with a model white dwarf atmosphere with $\log g = 9.0$ and $T_{eff} = 33,000\text{K}$. This fit to the FUSE spectrum provides independent confirmation of the results of Lake & Sion (2001) who also found that the far UV IUE spectra were dominated by a hot, massive white dwarf. The T_{eff} they derived with IUE for the white dwarf in SS Aur was 30,000K. This is surprising because it was widely felt that the white dwarf in SS Aur was not exposed, the system was disk-dominated in the far UV and could not be analyzed unambiguously.

In SS Aur, it is also highly significant that there is little evidence of an additional hot component other than a single temperature white dwarf photosphere. The absence of C III (1175 Å) absorption in the FUSE spectrum suggests the possibility that the white dwarf is deficient in carbon. If so, this could be an indication that past thermonuclear processing (ancient novae) depleted the carbon. This possibility is supported by the indication that the N-abundance in the SS Aur WD surface layers is elevated above solar. An alternative picture discussed by Gänsicke et al. (2003) suggest that the N/C anomaly seen in the dwarf novae BZ UMa, EY Cyg, 1RXS J232953.9+062814, and now CH UMa (Dulude & Sion 2002, 2004) may have its origin in a CV with an originally more massive donor star ($M_2 > 1.5M_\odot$) which survived thermal time scale mass transfer (Schenker et al. (2002) and references therein). In such a system, the white dwarf would be accreting from the peeled away CNO-processed core stripped of its outer layers during the thermal timescale mass transfer.

Our FUSE spectrum of RU Peg likewise reveals a very hot white dwarf in agreement with the analysis of the IUE archival spectra of RU Peg in quiescence. We find that $T_{eff} = 49,000\text{K}$ for the white dwarf, is very close to the T_{eff} derived by Sion & Urban (2002). However, the FUSE spectrum appears more complex than for SS Aur. There is evidence for a hot component. The best-fitting single temperature, high gravity, solar composition white dwarf models reveal a 49,000K white dwarf as the dominant source of the FUV continuum. The scale factors for the hot white dwarf fits yield distances of 230 pc and 260 pc, the latter value lying within the range of uncertainty of the new FGS parallax. We note however that although a hot single-temperature (50,000K) white dwarf agrees best with the far UV

observations, we cannot rule out that the far UV continuum could be produced by a cooler, slowly rotating white dwarf and a rapidly spinning, very hot accretion belt covering a small fraction of the white dwarf surface but providing the vast majority of the FUV flux.

4. Acknowledgements

This research was carried out with the support of NASA through FUSE grant NAG5-12067, and by NSF grant AST99-01955, both to Villanova University.

REFERENCES

- Dulude, M.J., & Sion, E.M. 2002, BAAS, 201, 401
- Dulude, M.J., & Sion, E.M. 2004, in preparation
- Friend, M.T., Martin, J.S., Smith, R.C., Jones, D.H.P. 1990, MNRAS, 246, 654
- Gänsicke, B.T., Szkody, P., De Martino, D., Beuermann, K., Long, K.S., Sion, E.M., Knigge, C., Marsh, T., Hubeny, I. 2003, ApJ, in press
- Harrison, T.E., McNamara, B.J., Szkody, P., McArthur, B.E., Benedict, G.F., Klemola, A.R., Gilliland, R.L. 1999, ApJ, 515, L93
- Johnson, J.J., Harrison, T.E., Howell, S.B., Szkody, P., McArthur, B.E., Benedict, G.F. 2003, BAAS, 202, 0702
- Hubeny, I. 1988, Comput. Phys. Comm., 52, 103
- Hubeny, I., & Lanz, T. 1995, ApJ, 439, 875
- Lake, J., & Sion, E.M. 2001, AJ, 122, 1632
- Schenker, K., King, A.R., Kolb, U., Wynn, G.A., Zhang, Z. 2002, MNRAS, 337, 1105
- Shafter, A. 1983, Ph.D Thesis, UCLA.
- Shafter, A., Wheeler, J., Cannizzo, J. 1986, ApJ, 305, 261
- Shafter, A., & Harkness, R.P. 1986, ApJ, 92, 658
- Sion, E.M., Cheng, F., Long, K., Szkody, P., Huang, M., Gilliland, R., Hubeny, I. 1995, ApJ, 439, 957
- Sion, E.M., & Urban, J. 2002, ApJ, 572, 456
- Stover, R. 1981, ApJ, 249, 673
- Wade, R. 1982, AJ, 87, 1558
- Warner, B. 1995, Cataclysmic Variable Stars (Cambridge: Cambridge University Press)

Table 1. System Parameters

| Object | RU PEG | SS AUR |
|--------------------------|--------|--------|
| Orbital Period (days) | 0.3746 | 0.1828 |
| V Magnitude (quiescence) | 12.6 | 14.5 |
| V Magnitude (outburst) | 9.0 | 10.5 |
| Recurrence Time (days) | 75-85 | 40-75 |
| Distance (pc) | 282 | 201 |

Table 2. SS Aur FUSE Line Measurements

| Center < Å > | Flux < erg/s/cm ² /Å > | EW < Å > | FWHM < Å > | Line | Identification < Å > |
|-----------------|--------------------------------------|-------------|---------------|--------|-------------------------|
| 910.9 | -5.6e-15 | 0.624 | 2.055 | S III | 911.7 |
| 916.7 | -4.9e-15 | 0.680 | 0.628 | Fe II | 915.97 |
| | | | | N II | 915.6, 916.0, 916.7 |
| 921.5 | -1.7e-14 | 2.297 | 3.166 | N IV | 922.0, 922.5, 923.2 |
| 927.5 | -3.4e-15 | 0.644 | 1.301 | ? | |
| 929.9 | -3.8e-15 | 0.649 | 0.734 | He II | 930.3 |
| 952.6 | -1.9e-14 | 3.303 | 4.169 | ? P IV | 950.7 ? |
| 964.5 | -1.7e-14 | 2.259 | 3.315 | ? | |
| 968.5 | -1.9e-14 | 2.506 | 4.717 | ? | |
| 980.6 | -3.6e-14 | 2.589 | 3.844 | N III | 979.9, 980.0 |
| 985.9 | -6.5e-14 | 4.771 | 3.015 | Cl IV | 985.0, 985.8, 986.1 |
| 994.0 | -5.3e-14 | 2.862 | 6.698 | Fe III | 993.1, 994.7, 995.1 |
| 1003.1 | -1.9e-14 | 1.260 | 3.268 | N III | 1002.85, 1003.21, |
| | | | | O III | 1003.35 |
| 1010.4 | -9.1e-15 | 0.788 | 1.995 | C II | 1010.1, 1010.4, |
| | | | | O III | 1010.5 |
| 1014.6 | -2.9e-14 | 2.522 | 4.092 | Cl III | 1015.0, |
| | | | | S III | 1015.5, 1015.8 |
| 1024.5 | -1.2e-13 | 10.98 | 17.35 | He II | 1025.4 |
| 1029.3 | -1.5e-14 | 1.281 | 2.755 | P IV | 1030.5 |
| 1037.2 | -1.8e-14 | 1.272 | 2.141 | C II | 1036.34, 1037.02 |
| 1065.7 | -6.3e-14 | 2.839 | 5.751 | S IV | 1066.6, |
| | | | | O IV | 1067.8, |
| | | | | Si IV | 1066.6 |
| 1078.0 | -2.7e-14 | 1.196 | 3.261 | S III | 1077.14, |
| | | | | N IV | 1078.71 |
| 1085.7 | -2.7e-14 | 1.213 | 5.331 | N II | 1085.5, 1085.7 |
| 1092.8 | -2.2e-14 | 0.977 | 2.438 | ? | |
| 1109.3 | -2.8e-14 | 1.393 | 2.889 | Si III | 1109.94, 1109.97 |
| 1113.3 | -1.8e-14 | 0.946 | 3.412 | Si III | 1113.20, 1123.23 |

Table 2—Continued

| Center < Å > | Flux < erg/s/cm ² /Å > | EW < Å > | FWHM < Å > | Line | Identification < Å > |
|-----------------|--------------------------------------|-------------|---------------|--------|-------------------------|
| 1122.7 | -1.6e-14 | 0.820 | 3.470 | Si IV | 1122.50 |
| 1128.8 | -1.7e-14 | 0.887 | 2.770 | Si IV | 1128.34 |
| 1144.0 | -4.9e-14 | 2.434 | 5.765 | Si III | 1144.3 |

Table 3. RU Peg FUSE Line Measurements

| Center < Å > | Flux < erg/s/cm ² /Å > | EW < Å > | FWHM < Å > | Line | Identification < Å > |
|-----------------|--------------------------------------|-------------|---------------|--------|--------------------------|
| 912.40 | -4.2e-13 | 6.941 | 9.226 | S III | 911.74? |
| 923.44 | -3.7e-13 | 1.19 | 2.361 | N IV | 923.22,923.68 |
| 930.58 | -1.7e-13 | 1.46 | 2.197 | He II | 930.34 |
| 933.84 | -9.7e-14 | 0.856 | 1.067 | He II | 933.40 |
| 938.63 | -1.4e-13 | 1.202 | 2.208 | He II | 937.39 |
| 965.25 | -1.3e-13 | 3.90 | 5.782 | Fe III | 967.19 ? |
| 972.49 | -1.4e-14 | 1.706 | 3.06 | He II | 972.11 |
| 986.12 | -1.7e-13 | 1.436 | 2.221 | Cl IV | 984.95,985.75,986.09 |
| 992.15 | -1.2e-13 | 1.116 | 1.646 | N III | 991.58, |
| | | | | He II | 992.36 |
| 1003.3 | -1.6e-13 | 1.477 | 3.109 | N III | 1002.85, 1003.21, |
| | | | | O III | 1003.35 |
| 1008.9 | -5.2e-14 | 0.523 | 0.646 | O III | 1008.10,1008.39, 1008.97 |
| | | | | Cl III | 1008.78 |
| 1013.6 | -9.3e-14 | 0.981 | 2.312 | ? | |
| 1025.4 | -2.1e-13 | 1.622 | 1.692 | He II | 1025.36 |
| 1031.9 | -2.4e-13 | 1.197 | 2.027 | P IV | 1030.5, 1033.11 |
| 1037.3 | -2.8e-13 | 1.7 | 2.082 | C II | 1036.34, 1037.02 |
| 1050.4 | -8.2e-13 | 6.349 | 11.98 | O III | 1050.4 |
| 1063.0 | -1.3e-13 | 1.117 | 1.418 | S IV | 1062.68 |
| 1073.5 | -9.0e-14 | 0.706 | 1.405 | S IV | 1072.99, 1073.52 |
| 1078.2 | -2.1e-13 | 1.676 | 3.342 | S III | 1077.14, |
| | | | | N IV | 1078.71 |
| 1096.4 | -3.5e-13 | 5.321 | 14.0 | ? | |
| 1109.3 | -1.1e-13 | 1.076 | 2.94 | Si III | 1109.94, 1109.97 |
| 1113.6 | -7.0e-14 | 0.686 | 1.883 | Si III | 1113.20, 1123.23 |
| 1160.6 | -8.9e-14 | 11.17 | 23.19 | O III | 1160.18 |
| 1176.1 | -1.6e-13 | 1.19 | 2.361 | C III | 1174.93, 1175.26, |
| | | | | | 1175.71,1175.99, 1176.37 |

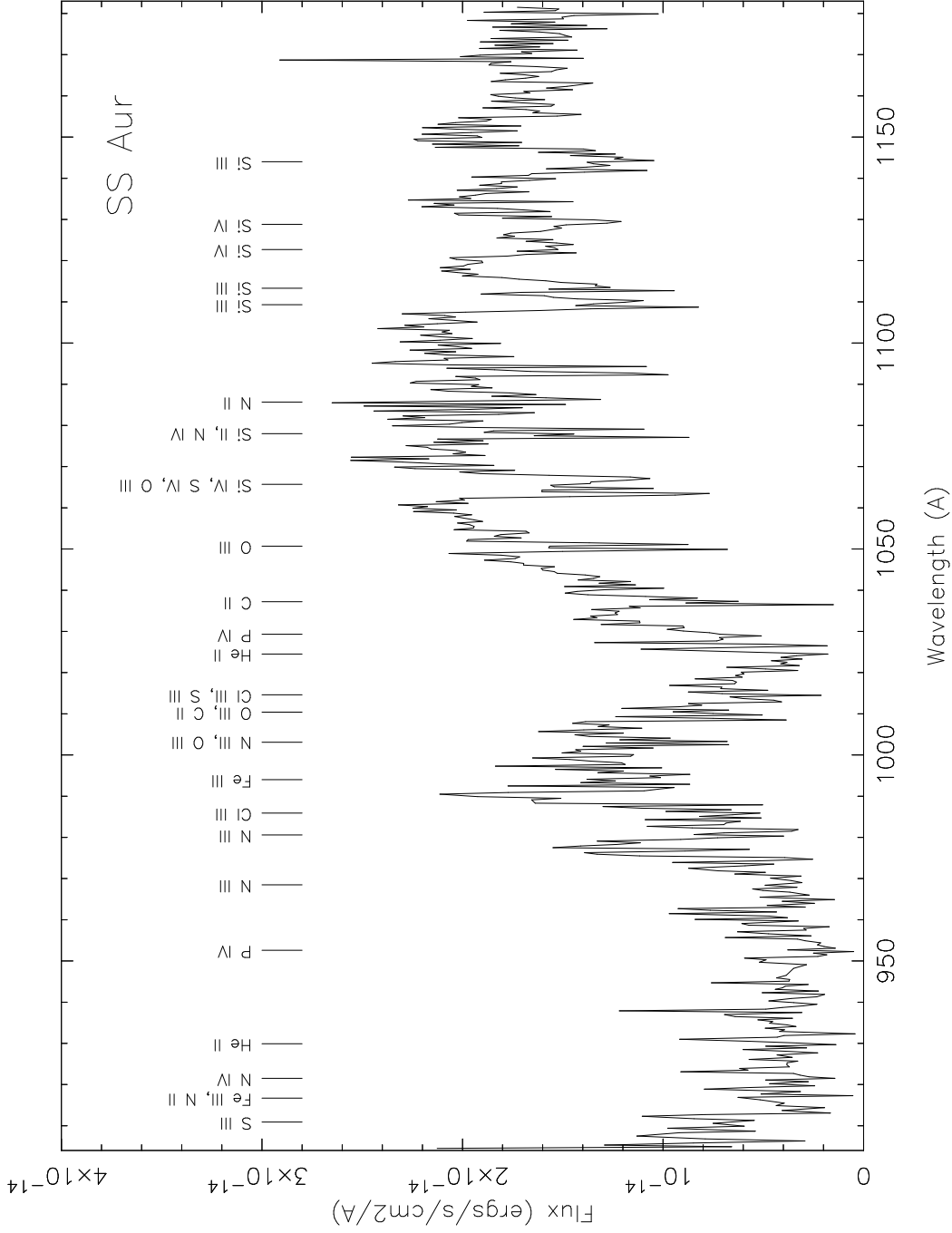


Fig. 1.— Line identification of the FUSE spectrum of SS Aur observed on February 13, 2002 (MJD52318). in quiescence, 28 days after outburst. The time-averaged spectrum was generated by combining the individual exposures and channels. The total exposure time was 14,513 s, through the FUSE LWRS aperture. The spectrum is binned here at 0.5 \AA for clarity.

Fig. 2.— Line identification of the FUSE spectrum of RU Peg observed on July 4th, 2002 (MJD52459). in quiescence, 60 days after outburst. The time-averaged spectrum was generated from a single exposure by combining the different channels. The total exposure time was 1,060 s, through the FUSE LWRS aperture. The spectrum is binned here at 0.5 Å for clarity.

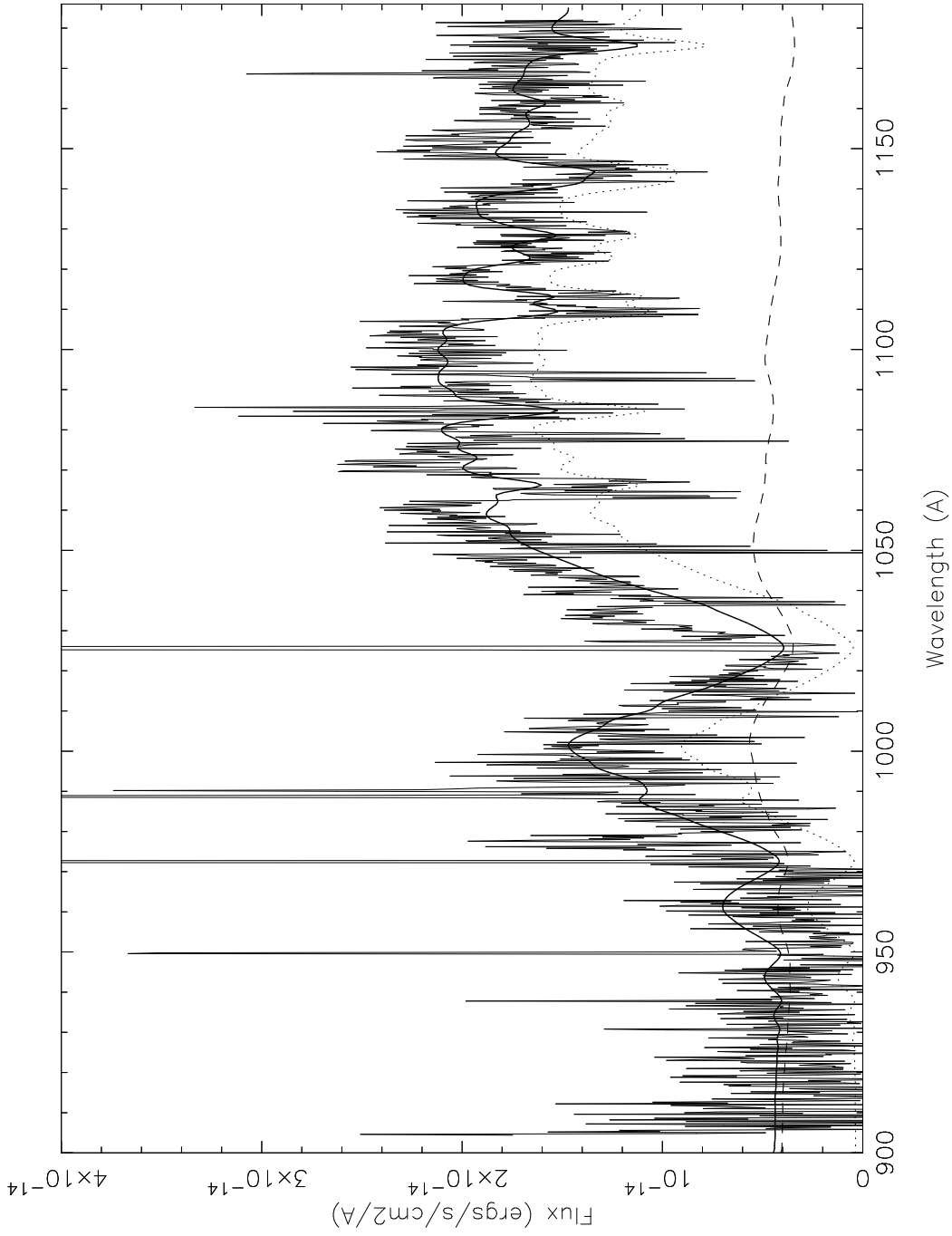


Fig. 3.— FUSE spectrum of SS Aur with the best fit model. Here the spectrum is binned at 0.1 \AA . The best fit model consists of a white dwarf atmosphere with $T_{eff} = 31,000\text{K}$.

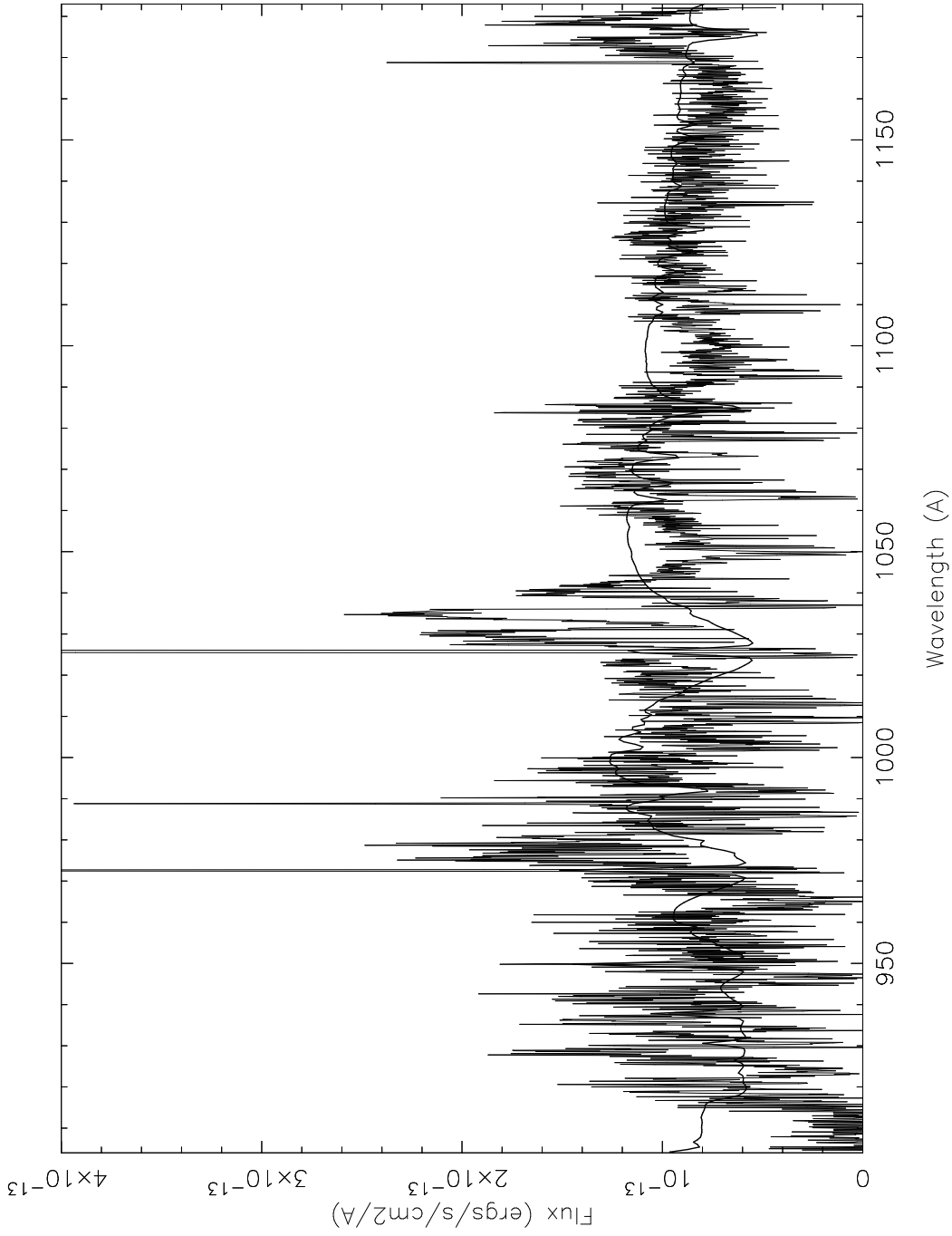


Fig. 4.— FUSE spectrum of RU Peg with the best fit model. Here the spectrum is binned at 0.1 \AA . The best fit model consists of a white dwarf atmosphere with $T_{eff} = 49,000\text{K}$.